

Electronic Supplementary Information (ESI):

**Hexagonal Boron Nitride supported mesoSiO₂-confined Ni Catalysts
for Dry Reforming of Methane**

*Yang Cao, Meirong Lu, Jianhui Fang, Liyi Shi and Dongsong Zhang**

*Department of Chemistry, Research Center of Nano Science and Technology, Shanghai University,
Shanghai 200444, P. R. China.*

Fax: 86 21 66136079; E-mail: dszhang@shu.edu.cn

Experimental section

1. Reagents and materials

The hexagonal boron nitride (h-BN) was purchased from Saint-Gobain Ceramic Materials and the other chemical materials were purchased from Sinopharm Chemical Reagent Company China. Deionized water was used for all applications.

2. Catalyst preparation

Synthesis of Ni/BN@mSiO₂ catalyst

The h-BN (0.4 g) and Ni precursor (Ni(NO₃)₃·6H₂O 0.15g) were dispersed in the mixture solution of ethanol (120 mL) and deionized water (160 mL) using a sonic bath for 3 h. Then the cetyltrimethylammonium bromide (CTAB 0.6 g) and concentrated ammonium hydroxide (NH₃·H₂O 28 wt% 1.8 mL) were added respectively under vigorous stirring. After being stirred 30 min, a mixture solution of ethanol solution (2.4 g) and tetraethyl orthosilicate (TEOS 0.6g) was added into the solution dropwise in 30 min under vigorous stirring. As the reaction proceeds at room temperature, a homogeneous pale green colloidal solution was obtained under continuous stirring. After stirring for 6 h, washed the samples with deionized water and ethanol, then collected by centrifugation and finally dried overnight at 90 °C. The as-prepared samples were calcined at 600 °C for 4 h under air atmosphere and reduced under the H₂ at 800 °C, the obtained catalysts denoted as Ni/BN@mSiO₂. The loading of Ni was at 5.31 wt% determined by ICP analysis.

Synthesis of Ni/mSiO₂@BN catalyst

The synthesis of Ni/mSiO₂@BN catalyst mainly includes two aspects, the synthesis of mSiO₂@BN support and the impregnation process of Ni species. The synthesis of mSiO₂@BN support is similar to that for mesoSiO₂ coating, except the addition of Ni precursor. The h-BN (0.4 g) were dispersed in ethanol solution using a sonic bath for 3 h. Then the CTAB (0.6 g) and NH₃·H₂O (28 wt% 1.8 mL) were added respectively under vigorous stirring. After being stirred 30 min, a mixture solution of ethanol solution (2.4 g) and TEOS (0.6g) was added into the solution dropwise in 30 min under vigorous stirring. After stirring for 6 h, washed the samples with deionized water and ethanol, then collected by centrifugation and finally dried overnight at 90 °C and the support were obtained by the calcination at 600 °C for 4 h. Then, a certain amount of Ni precursor (Ni(NO₃)₃·6H₂O) was impregnated on the obtained BN@SiO₂ support using a sonic

bath for 3 h and a rotary evaporator. Finally, the as-prepared sample was calcined and reduced under the same conditions as above mentioned. The obtained catalyst was denoted as Ni/mSiO₂@BN and the loading of Ni was at 6.23 wt % determined by ICP analysis.

Synthesis of Ni/BN catalyst and Ni/SiO₂ catalyst

The Ni/BN catalyst and Ni/SiO₂ catalyst were prepared by impregnation process as above mentioned. The supports were h-BN and SiO₂ respectively. The loading of Ni over the Ni/BN catalyst and Ni/SiO₂ catalyst were at 5.60 wt % and 6.43 wt %, respectively.

3. Characterization

Materials Characterization

The detailed morphology of samples was performed using transmission electron microscopy (TEM) and high resolution TEM (HRTEM) on JEOL JEM-200CX. The microscope was also equipped with energy dispersive X-ray spectroscopy (EDS) detector for elemental distribution of the catalyst. Elemental composition was obtained by inductively coupled plasma-atomic emission spectrometer (ICP-AES). The hydrogen chemisorption and N₂ adsorption-desorption isotherm were carried out on Quantachrome instrument. The specific surface areas and pore size distribution of the catalyst were obtained using BET equation and BJH method, respectively. The XRD pattern was carried out on a Rigaku D/MAX-RB X-ray diffractometer with Cu K α radiation. X-ray photoelectron spectroscopy (XPS) was performed using a RBD upgraded PHI-5000C ESCA system.

Surface Adsorption and Desorption

The H₂-temperature programmed reduction (H₂-TPR) was carried out to demonstrate the redox ability of the catalysts. First, the catalysts (80 mg) were pretreatment at 300 °C for 30 min under the N₂ atmosphere, and then reduced in 10 vol% H₂ of N₂ (30mL·min⁻¹) atmosphere from room temperature to 800°C at a ramp rate of 10 °C·min⁻¹.

In situ diffuse reflectance infrared transform spectroscopy (DRIFTS) was performed on a Nicolet 6700 spectrometer with a Harrick Scientific DRIFT cell and a mercury-cadmium-telluride (MCT) detector to illustrate the study of the catalysts behavior during the DRM reaction. Firstly, the catalysts were purged with N₂ (50 mL·min⁻¹) at 300 °C, then cooled down to get the background spectrum. In a typical experiment, the catalysts were exposed to CO₂ (45 mL·min⁻¹) atmosphere at 500 °C for 1 h and then stop the adsorption of CO₂. Next, introduce CH₄ (45

mL·min⁻¹) steam to illustrate the transformation of the intermediate species with CH₄ introducing. In comparison, treat the CO₂ pre-adsorbed catalyst with flowing CH₄ stream, and also treat the CH₄ pre-adsorbed catalyst with flowing CO₂ stream, to examine the active species. In another experiment designed to illustrate the process of the DRM reaction, the catalysts were exposed to CO₂ (45 mL·min⁻¹) and CH₄ (45 mL·min⁻¹) for 1 h at 500 °C. The DRM reaction at 500 °C for 1 h has been measured for 3 cycles. Of each cycle the catalysts were purged with N₂ (50 mL·min⁻¹) at 500 °C for 30 min.

The thermogravimetric (TG) was performed on NETZSCH STA 449 F1 to illustrate the deposited carbon. The carbonized catalysts were heated in 40 vol% O₂ of N₂ flow (30mL·min⁻¹) from room temperature to 800 °C at a ramp rate of 10 °C·min⁻¹.

Catalyst test

The catalytic tests were conducted in a quartz fixed-bed tubular reactor loaded with 120 mg catalysts. The feed, a mixture of CH₄ and CO₂ (CO₂/CH₄=1) was introduced at a gas hourly space velocity (GHSV) of 15000 mL·(gh)⁻¹. The products were analyzed by a gas chromatograph (GC) equipped with thermal conductivity detector (TCD). The catalytic stability was carried out at 750 °C for 20 h and 100 h, respectively. The catalytic activity was carried out and the temperature range of the test is from 450 °C to 800 °C.

The thermodynamic equilibrium is calculated by Equilibrium Composition Block of HSC software, version 6.0 consisting of DRM and RWGS reaction.

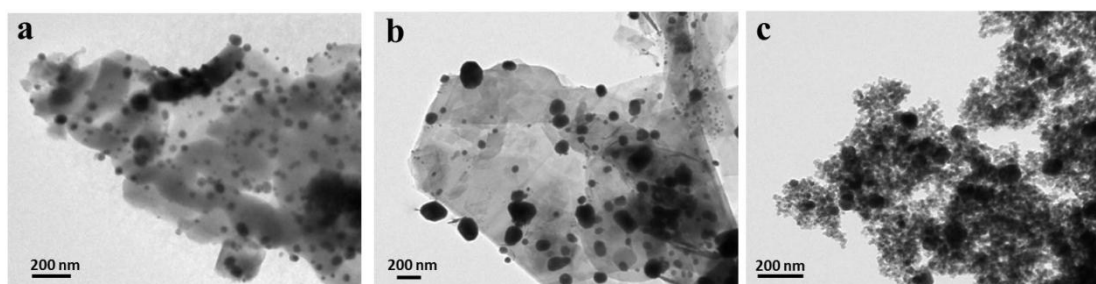


Fig. S1 TEM images of the a) Ni/mSiO₂@BN; b) Ni/BN; c) Ni/SiO₂ catalysts.

For the Ni/mSiO₂@BN catalyst, the Ni particles mainly loaded on the surface of mesoSiO₂ coating. In addition, the Ni particle sizes of the Ni/mSiO₂@BN, Ni/BN and Ni/SiO₂ catalysts are much bigger than the Ni/BN@mSiO₂ catalyst.

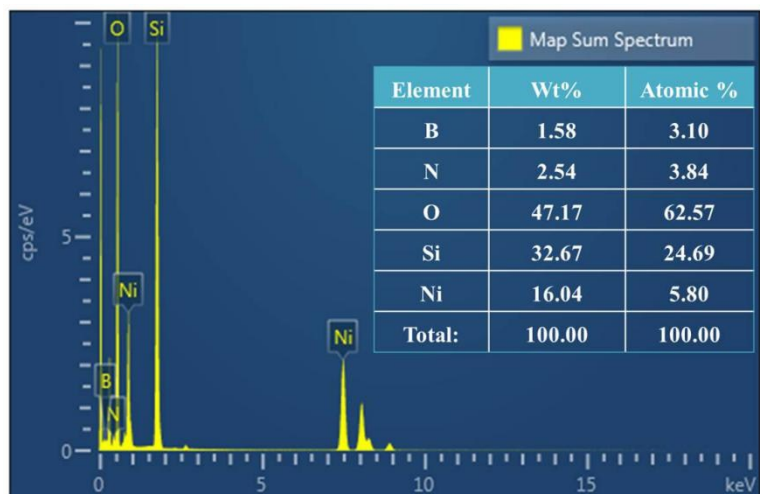


Fig. S2 EDX analyses in Fig. S2 showed that the body of the Ni/BN@mSiO₂ catalyst was composed of elements B, N, O, Ni and Si and the corresponding atom content were shown in the inserted table.

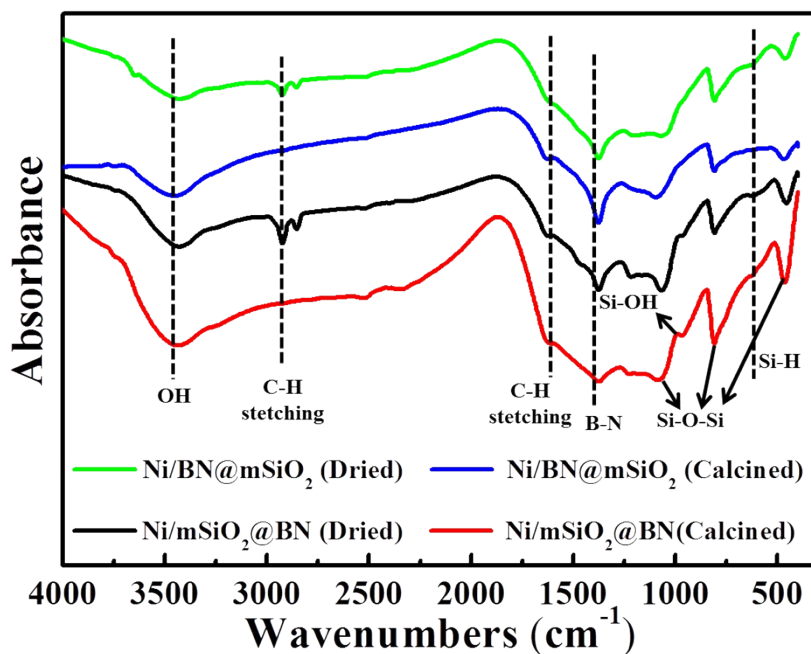


Fig. S3 FT-IR spectra of the samples.

The surface properties of the dried and calcined samples were determined by FT-IR in Fig. S3. The band at 3437 cm^{-1} can be assigned to the H-bonded OH groups and the band at 1380 cm^{-1} suggested the existence of the BN species.¹ The C-H bands at 2926 cm^{-1} and 1638 cm^{-1} were detected over the dried samples corresponded to the treatment of an impregnation via ethanol. In addition, the Si-OH and Si-H bands at 956 cm^{-1} and 616 cm^{-1} were observed.² Meanwhile, the Si-O-Si bands at 1056 cm^{-1} , 796 cm^{-1} and 435 cm^{-1} were strong, on the one hand, illustrating the interaction of the silica species and h-BN nanosheets. Because the h-BN supported Ni species could interact with H-bonded Si-OH species, forming the Si-OH coating. These findings further confirm the structure of the BN-templated conjugated mesoSiO₂ species.

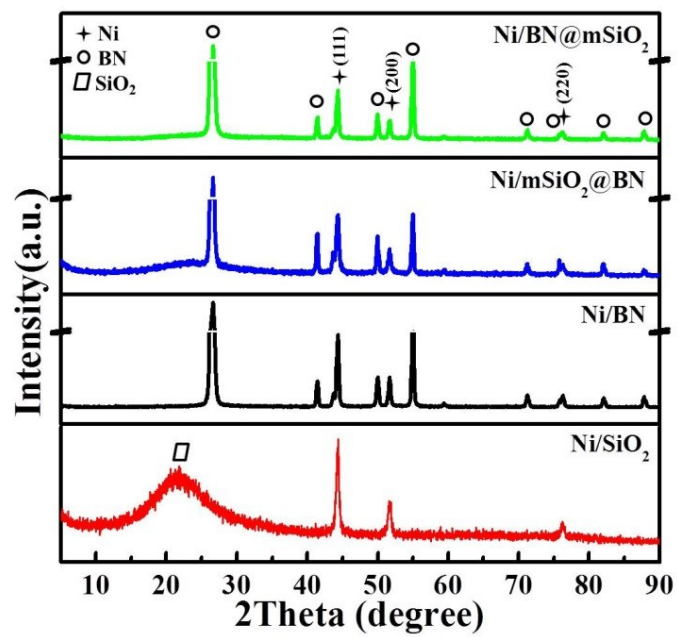


Fig. S4 XRD patterns of the reduced catalysts.

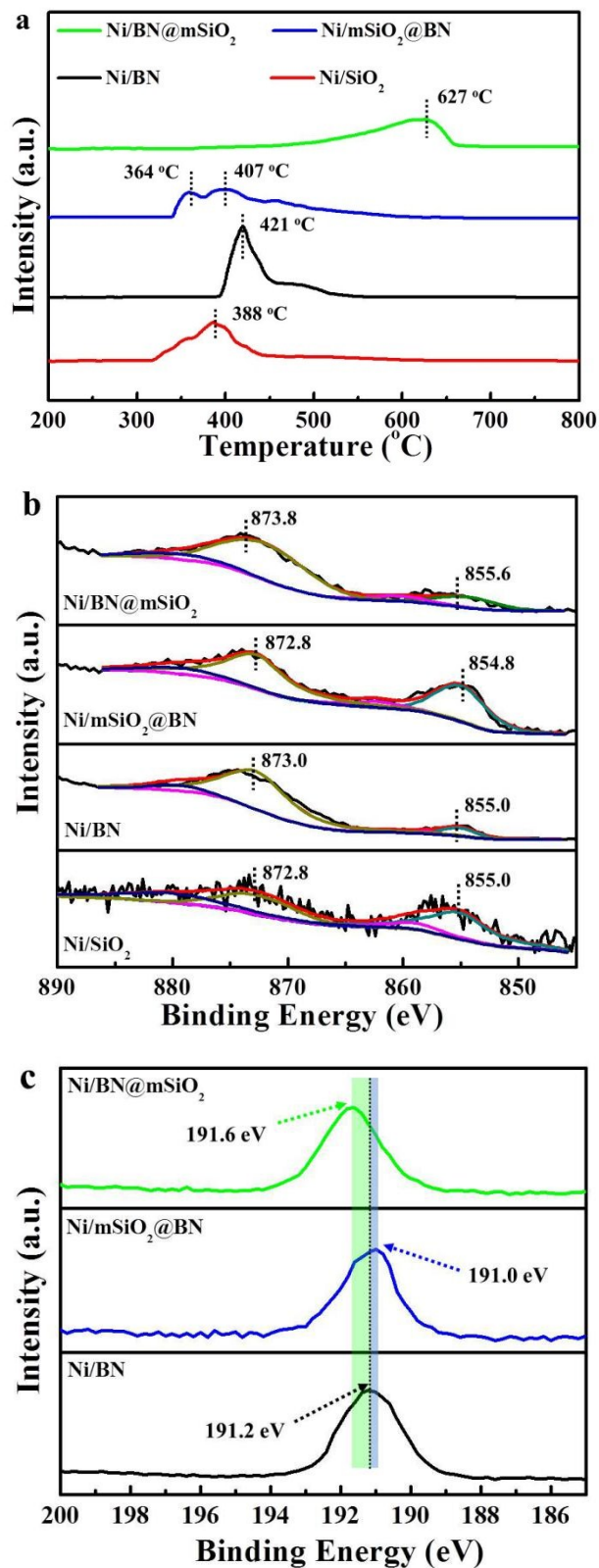


Fig. S5 a) H₂-TPR profiles, b) Ni 2p XPS spectra and c) B 1s XPS spectra of the reduced catalysts.

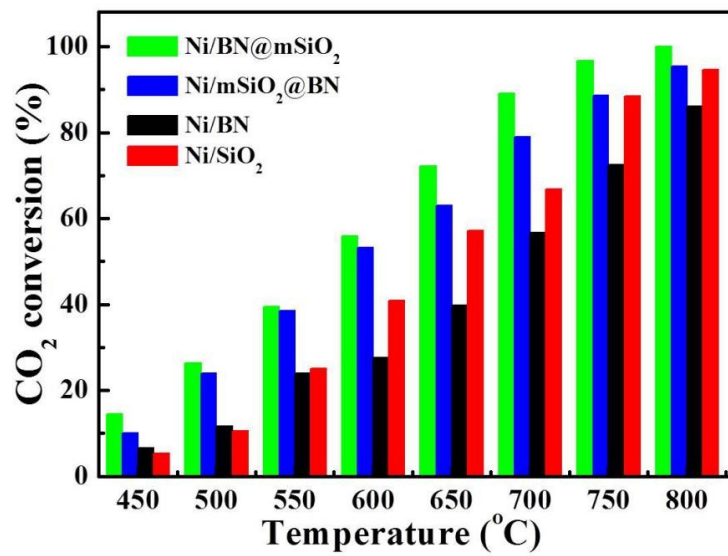


Fig. S6 Temperature dependence of CO₂ conversions over the reduced catalysts.

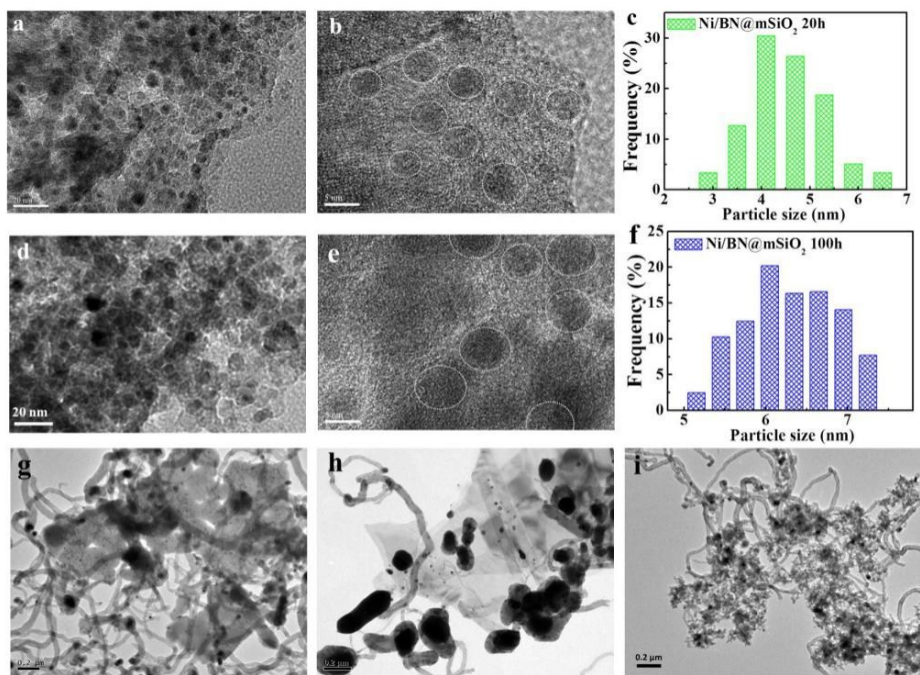


Fig. S7 a) TEM, b) HRTEM images, c) the size distribution of Ni particles after 20 h test and d) TEM, e) HRTEM images, f) the size distribution of Ni particles after 100 h stability test over the Ni/BN@mSiO₂ catalyst. TEM images of g) Ni/mSiO₂@BN; h) Ni/BN; i) Ni/SiO₂ catalysts after 20 h stability test.

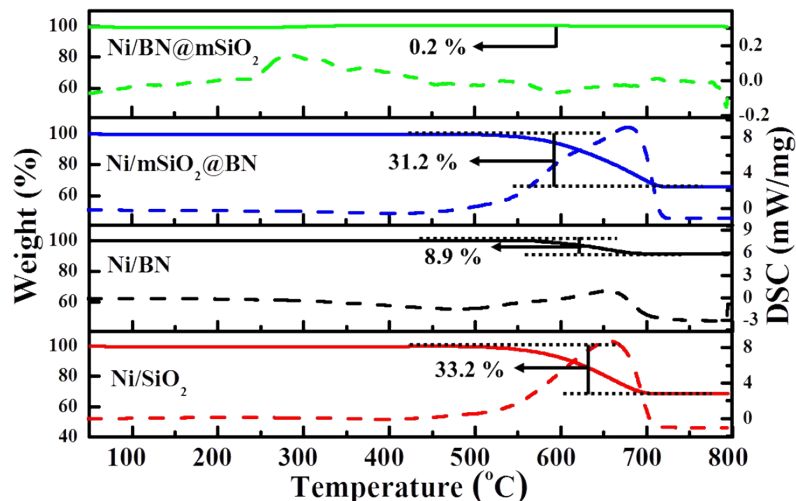


Fig. S8 TG profiles and DSC curves of the spent catalysts after 20 h stability test.

Fig. S8 shows the TG profiles and DSC curves of the spent catalysts. TG profiles can illustrate the amount of deposited carbon and DSC curves can demonstrate the types of deposited carbon. As DRM reaction is operated at high temperatures, the formation of coke by means of CH_4 decomposition is favored, and CO disproportionation is less favored at such temperatures. Previous studies reported that CH_4 decomposition mainly generates highly reactive carbon species C_α . Most of the C_α species can be gasified by reactions with H_2O , CO_2 , or hydrogen, but some are converted into less active C_β . The C_β would be further gasified, but may encapsulate on the surface or encapsulate the Ni species, leading to the deactivation of the catalysts. Therefore, coke formation is a result of the balance between the coke formation and gasification. Notably, DSC curve of the Ni/BN@mSiO_2 catalyst shows a peak ranged from 200 °C to 300 °C which can be assigned to the active carbon species. While, DSC curves of the $\text{Ni/mSiO}_2@BN$, Ni/BN and Ni/SiO_2 show a broad peak ranged from 550 °C to 700 °C which can be assigned to the carbon nanotube and graphite carbon. These types of carbon can deposit on the surface of Ni sites, leading to the deactivation of the catalysts.

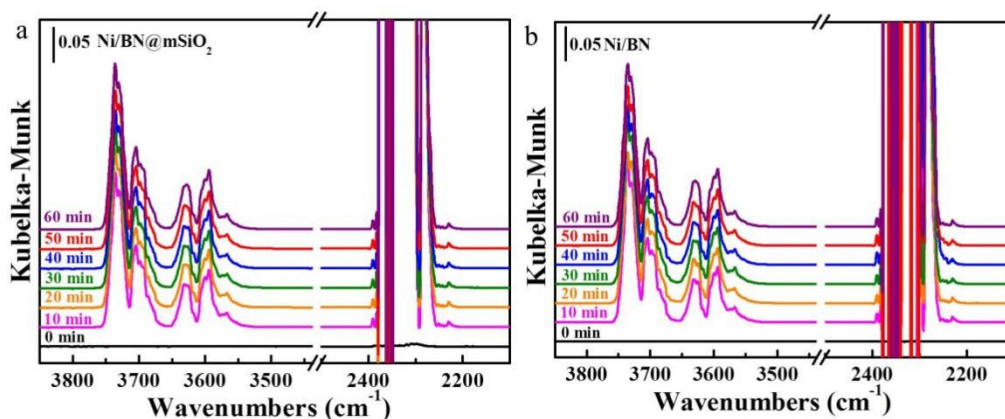


Fig. S9 *In situ* DRIFTS of a) the Ni/BN@mSiO₂ catalyst and b) the Ni/BN catalyst after the catalysts were pre-adsorbed CO₂ at 500 °C for 1h.

First, the catalysts were pre-adsorbed by CO₂ at 500 °C for 1 h, the *in situ* DRIFTS were collected as presented in Fig. S9. The strong feature at 2350-2280 cm⁻¹ region can be attributed to the adsorbed CO₂ and the band at 3550-3750 cm⁻¹ region can be assigned to the OH vibrations of the surface OH groups linked by H-bonds.^{1a, 3} It can be noticed that no feature peaks were detected before the adsorption of CO₂ and the OH groups appeared following the introduction of CO₂. Both theoretical calculations and experimental research have reported that h-BN as hydrogen adsorbent showed a high H₂ uptake capacity *via* chemisorption or physisorption.⁴ After the reduction treatment in the H₂ atmosphere, the h-BN support can bound to amount of H atoms possibility but it is difficult to detect the strongly bounded H atoms. In addition, the h-BN support can be able to capture CO₂ effectively.⁵ Therefore, the activation of CO₂ can occur on both active Ni sites and Ni-BN interface, the formed active species can react with the surface B-H to form B-OH intermediates. Both the adsorbed CO₂ species and B-OH intermediates can be clearly observed on the Ni/BN@mSiO₂ and Ni/BN catalysts. The synergistic effect of the active Ni sites and the Ni-BN interface can effectively promote the activation of CO₂ and CH₄ during the DRM reaction.

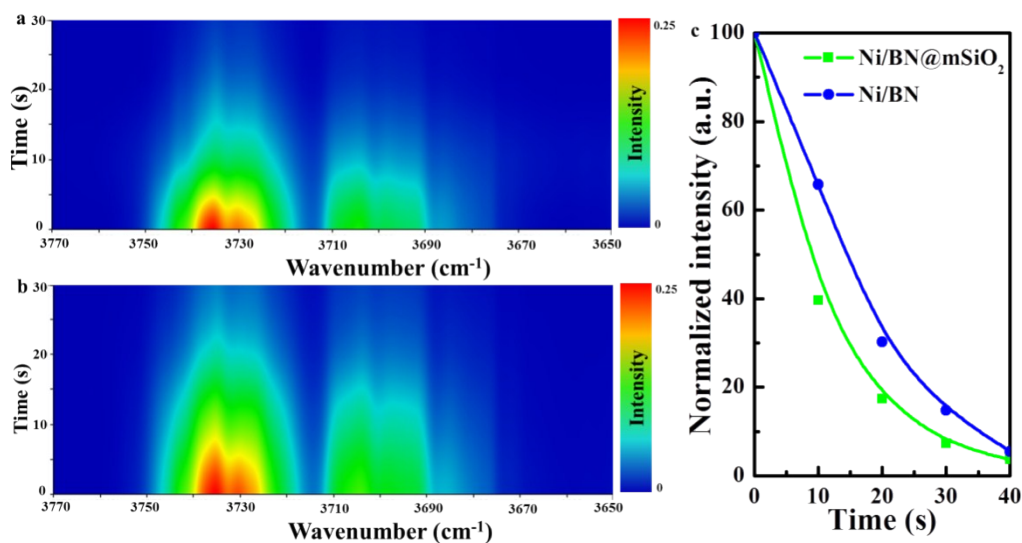


Fig. S10 Evolution of *in situ* DRIFTS after CO₂ adsorption at 500 °C. *In situ* DRIFTS of transient reactions over a) the Ni/BN@mSiO₂ catalyst and b) the Ni/BN catalyst after the catalysts were exposed to CH₄ species; (C) consumption of B-OH species upon passing CH₄ over the Ni/BN@mSiO₂ and Ni/BN catalysts.

As shown in Fig. S10a-b, the intensity of the B-OH peaks over the Ni/BN@mSiO₂ catalyst decreases at a more rapid rate compared with the Ni/BN catalyst. The normalized intensity of the B-OH intermediates changed with time over the Ni/BN@mSiO₂ and Ni/BN catalysts are shown in Fig. S10c. Of the B-OH peaks at 3735 cm⁻¹, 3704 cm⁻¹, 3626 cm⁻¹ and 3592 cm⁻¹, the main peak at 3735 cm⁻¹ is used to illustrate the reactivity of B-OH intermediates over the different catalysts. The intensity of B-OH intermediates decreases as time going by, suggesting that the adsorbed B-OH species can react with CH₄ and contributes to the DRM activity. We supposed that the active CH_x species derived from CH₄ decomposition can react with OH species, and then form the CH_xO species on the surface of support. Specially, this reaction process can contribute to the transport of the CH_x species from the Ni sites to the surface of support, providing more Ni sites for the CH₄ activation. Therefore, the decreased B-OH species can be due that the reaction between the CH_x species derived from CH₄ decomposition and B-OH species.

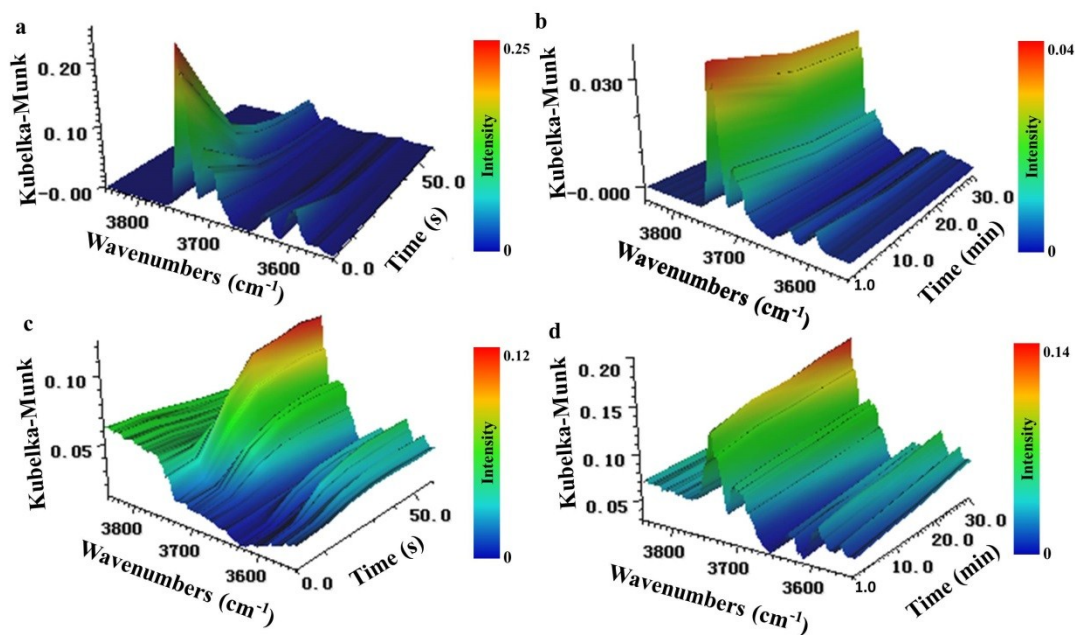


Fig. S11 Evolution of *in situ* DRIFTS over the Ni/BN@mSiO₂ catalyst after CO₂ adsorption at 500 °C with flowing CH₄ stream for a) 1 min and b) 30 min; after CH₄ adsorption at 500 °C with flowing CO₂ stream for c) 1 min and d) 30 min.

The Ni/BN@mSiO₂ catalyst was pre-adsorbed CO₂ at 500 °C for 1 h and then introduce the CH₄ stream simultaneously (Fig. S11a). The intensity of the B-OH peaks over the Ni/BN@mSiO₂ catalyst decreases rapidly with flowing CH₄ stream, suggesting that the adsorbed B-OH species can react with CH₄ as discussed. Notably, the intensity of the B-OH species maintains after 1 min (Fig. S11b), which is a result of the balance between the consumption and generation of B-OH species. In comparison, the Ni/BN@mSiO₂ catalyst was pre-adsorbed CH₄ at 500 °C for 1 h and then introduce the CO₂ stream simultaneously. As shown in Fig S11c, B-OH peaks do not appear after the adsorption of CH₄ for 1 h. While the B-OH peaks appears and increased rapidly with flowing CO₂ stream, and the intensity of B-OH species also maintains after 1 min (Fig. S11d). In addition, it can be notice that the intensities of B-OH species with different pre-adsorption are different. The CH₄ pre-adsorbed catalyst with flowing CO₂ stream shows the higher intensity of B-OH species. It may be due to that CH₄ decomposition can occur on the Ni sites and generate H species and H₂. While, h-BN as hydrogen adsorbent can absorb abundant H and H₂ species, contributing to the formation of B-OH species.

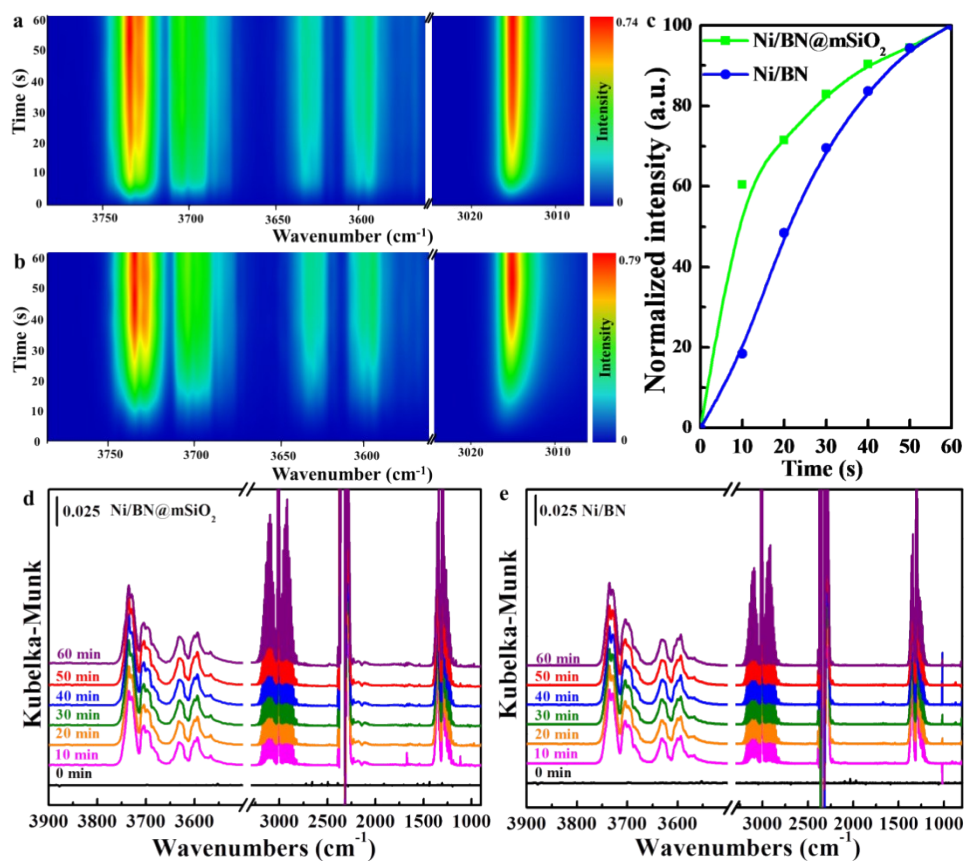


Fig. S12 *In situ* DRIFTS of the DRM reaction at 500 °C for 1 min the over a) Ni/BN@mSiO₂ and b) Ni/BN catalysts; c) formation of active species upon passing CH₄ and CO₂ over the Ni/BN@mSiO₂ and Ni/BN catalysts; *in situ* DRIFTS of the DRM reaction at 500 °C for 1 h over the d) Ni/BN@mSiO₂ catalyst and e) Ni/BN catalyst.

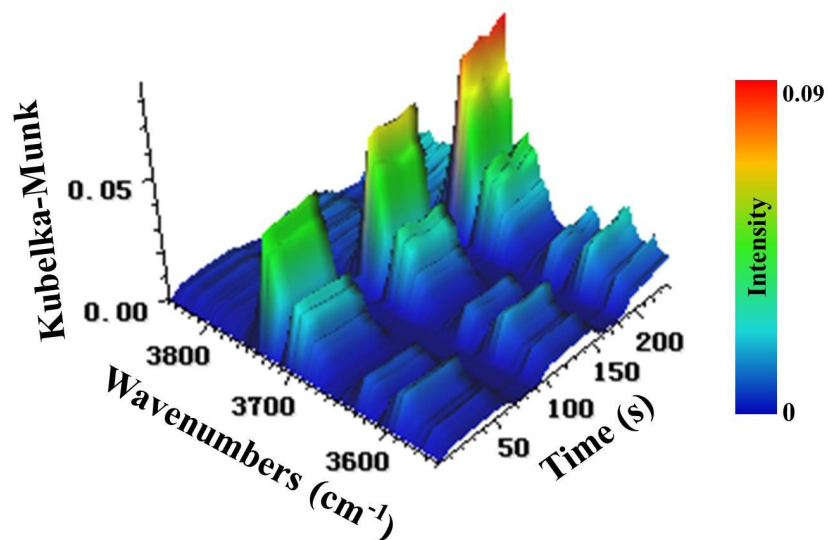


Fig. S13 *In situ* DRIFTs of three cycles of the DRM reaction at 500 °C.

Three cycles of DRM reaction have been examined to illustrate the regenerability of B-OH species. As shown in Fig. S13, the B-OH species can be formed with flowing CO₂ and CH₄ stream, and the B-OH peaks disappear with N₂ purging. Notably, the B-OH species can be regenerated on the surface of the Ni/BN@mSiO₂ catalyst with flowing CO₂ and CH₄ stream for each cycle.

Table S1. Surface Ni exposure from H₂ chemisorption

Catalysts	Ni dispersion
Ni/BN@mSiO ₂	9.74 %
Ni/mSiO ₂ @BN	1.32 %
Ni/SiO ₂	1.15 %

The Ni dispersions of the Ni/BN@mSiO₂, Ni/mSiO₂@BN and Ni/SiO₂ catalysts are 9.74 %, 1.32 % and 1.15 %, respectively. But the Ni dispersion of the Ni/BN catalyst can not be measured. Both theoretical calculations and experimental research have reported that h-BN as hydrogen adsorbent showed a high H₂ uptake capacity via chemisorption or physisorption. After the reduction treatment in the H₂ atmosphere, the h-BN support can bound to amount of H atoms possibility. Therefore, the high H₂ uptake capacity of the h-BN can influence the measurement of the hydrogen chemisorption.

Table S2. TOF value obtained from H₂ chemisorption

Time	Ni ^a (wt %)	Ni Dispersion ^b (%)	Conversion (CH ₄) ^c (%)	TOF _{CH₄} ^d (h ⁻¹)
15 min	5.31	9.74	13.82	3782
360 min		9.02	12.07	3565

Condition: 50mg of catalysts, CH₄:CO₂ = 1:1, 45 mL/min per reactor, Temperature: 550 °C.

^a Determined by ICP

^b Determined by H₂ chemisorption

^c CH₄ conversion at 15 min and 360 min of the DRM reaction

^d In mole_{CH₄}.h⁻¹.mole⁻¹surf.Ni

Reference

- 1 (a) Y. Saih, K. Segawa, *Appl. Catal., A*, 2009, **353**, 258-265; (b) G. Postole, A. Gervasini, M. Caldararu, B. Bonnetot, A. Auroux, *Appl. Catal., A*, 2007, **325**, 227-236.
- 2 X. Lv, J.-F. Chen, Y. Tan, Y. Zhang, *Catal. Comm.*, 2012, **20**, 6-11.
- 3 (a) S. Sinthika, E. M. Kumar, V. J. Surya, Y. Kawazoe, N. Park, K. Iyakutti, R. Thapa, *Sci. Rep.*, 2015, **5**, 17460; (b) T. Harada, F. Simeon, E. Z. Hamad, T. A. Hatton, *Chem. Mater.*, 2015, **27**, 1943-1949.
- 4 (a) G. Zhao, Y. Li, C. Liu, Y. Wang, J. Sun, Y. Gu, Y. Wang, Z. Zeng, *Int. J. Hydrogen Energy*, 2012, **37**, 9677-9687; (b) H. Zhang, C.-J. Tong, Y. Zhang, Y.-N. Zhang, L.-M. Liu, *J. Mater. Chem., A*, 2015, **3**, 9632-9637; (c) M. Samolia, T. J. D. Kumar, *J. Phy. Chem., C*, 2014, **118**, 10859-10866.
- 5 (a) H. Choi, Y. C. Park, Y. H. Kim, Y. S. Lee, *J. Am. Chem. Soc.*, 2011, **133**, 2084-2087; (b) Q. Sun, Z. Li, D. J. Searles, Y. Chen, G. M. Lu, A. Du, *J. Am. Chem. Soc.*, 2013, **135**, 8246-8253.